Geophysical Research Letters

Supporting Information for

A 21st Century Warming Threshold for Sustained Greenland Ice Sheet Mass Loss

B. Noël[1]*, L. van Kampenhout[1]*,
J. T. M. Lenaerts[2], W. J. van de Berg[1], M. R. van den Broeke[1]

[1] Institute for Marine and Atmospheric Research, Utrecht University
[2] Department of Atmospheric and Oceanic Sciences, University of Colorado Boulder

**Contributed equally to this work*

Contents of this file

Introduction

This document supplements the main manuscript in the following ways:

- Additional methodology and background information: Text S1, Figure S1, Figure S4, Table S3, Table S4.
- Additional results: Figure S2 to S5, Table S1 and S2.

Text S1. Extended methodology

CESM2 elevation classes and SMB. Over ice sheets, CESM2 employs multiple elevation classes to downscale GrIS SMB from the 1º (~111 km) atmosphere grid to a 4 km ice sheet grid as described in Van Kampenhout et al. (2020). Within each grid cell, up to 10 elevation classes are defined with weighting based on a high-resolution topographic map. Each elevation class maintains its own snow pack and downscales 2-m temperature, humidity, downwelling longwave radiation and precipitation phase based on fixed lapse rates. Elevation class variables are aggregated on the 1º grid using the topographic weights, and SMB is interpolated towards the high-resolution ice sheet grid. CESM2 implements a relatively sophisticated treatment of snow albedo (Dang et al., 2019) and firn processes (Van Kampenhout et al., 2017) and has been shown to realistically simulate GrIS climate and SMB (Van Kampenhout et al., 2020).

Dynamical and statistical downscaling. We use the regional atmospheric climate model (RACMO2.3p2) at 11 km spatial resolution to dynamically downscale CESM2 over the greater Greenland area. RACMO2 is forced at its lateral boundaries by one historical (1950-2014; Noël et al., 2020) and one SSP5-8.5 (2015-2099) member of CESM2. Forcing consists of temperature, pressure, specific humidity, wind speed and direction being prescribed in a 24 grid-cell-wide relaxation zone at the 40 model atmospheric levels every 6 hours. Sea ice extent and temperature are also prescribed from CESM2 on a 6-hourly basis. Using elevation dependence, daily RACMO2 outputs are further statistically downscaled to a 1 km resolution grid, using the GIMP digital elevation model and ice mask (Howat et al., 2014). We use a 500 m Moderate Resolution Imaging Spectroradiometer (MODIS) albedo product (http://dx.doi.org/10.5067/MODIS/MCD43A3.006) to correct melt and runoff for biases in bare ice albedo at the GrIS margins on the 11 km grid. Details about the RACMO2 settings and the statistical downscaling procedure are provided in Noël et al. (2018) and results for present-day are presented in Noël et al. (2020). Due to high computational costs, RACMO2 was forced by one CESM2 historical member (1950-2014) and one high-end warming scenario (2015-2100, SSP5-8.5). To sample other warming trajectories, we included other CESM2-based CMIP6 scenarios (10 members; SSP1-2.6 to SSP5-8.5). We find high correlation between the downscaled RACMO2.3p2-CESM2 and the corresponding native CESM2 SSP5-8.5 projection ($R^2 = 0.97$; Fig. S1a), enabling us to predict meaningful GrIS SMB under various warming scenarios after applying a small linear correction.

$$X_{corr} = a \,.\, X_{CESM2} + b$$

where X_{corr} is the corrected CESM2 SMB component (X), X_{CESM2} the SMB component derived from the native CESM2 grid, a and b are the slope and intercept of the linear regression calculated for individual SMB components between RACMO2.3p2-CESM2 and the native CESM2 outputs (Fig. S1). Figure 1a shows that the resulting CESM2 reconstructions under independent SSP5-8.5 scenarios (3 members; red) agree well with the downscaled product, highlighting the robustness of the approach.

Ice-sheet wide SMB is calculated by integrating specific SMB over the contiguous ice sheet. An SMB uncertainty of 48 Gt yr^{-1} is estimated for the downscaled product by summing the mean accumulation (20.5 mm w.e.) and ablation (180 mm w.e.) biases (b) over the long-term (1950-2014) accumulation (1,521,400 km^2) and ablation (179,400 km^2) zone area A of the GrIS:

$$\sigma = \sqrt{(b^{abl.} \times A^{abl.})^2 + (b^{acc.} \times A^{acc.})^2}$$

Assuming that these biases remain valid for a high-end warming scenario (SSP5-8.5), we obtain a 72 Gt yr^{-1} SMB uncertainty for the period 2051-2055, i.e. when the SMB = 0 threshold is passed. In that period the accumulation and ablation zones cover an area of 1,345,400 and 348,600 km^2 respectively.

T_{GrIS} anomaly and uncertainty. Greenland temperature (T_{GrIS}) is defined as the average 2-m air temperature over grid points with at least 50% land cover between 72 ºW and 12 ºW longitude, 59 ºN and 85 ºN latitude. It is calculated per model using each model's native land-ocean mask. Hence, CMIP climate models that do not provide this mask had to be excluded. For CESM2, the T_{GrIS} anomaly is calculated with respect to the ensemble mean of the twelve historical CESM2 members for the period 1850-1899. A T_{GrIS} uncertainty of 0.3 ºC is estimated using the quadratic regression shown in Fig. 1b and the SMB uncertainty of 48 Gt yr^{-1}, derived from the historical CESM2-forced RACMO2 simulation at 1 km (Noël et others, 2019). Using the SMB uncertainty of 72 Gt yr^{-1} predicted for 2051-2055, we estimated a T_{GrIS} uncertainty of 0.5 ºC. Since the resulting uncertainty difference of 0.2 ºC is small compared to the absolute value of the threshold (4.5 ºC), we kept the T_{GrIS} uncertainty at 0.3 ºC that is derived from a direct comparison between modelled and observed SMB. For the CMIP models, the T_{GrIS} anomaly is calculated with respect to the same reference period (1850-1899) in their historical run. Some CMIP models start later than 1850 and therefore have a shorter reference period, but never shorter than 39 years.

T_{GrIS} from reanalysis. Figure 3 compares T_{GrIS} anomalies derived from the hybrid reanalysis product (Table A1) to those from the CMIP5 and CMIP6 ensemble. The reanalysis anomalies are calculated with respect to the baseline period 1958-1977, and offset by the accumulated warming in that same period with respect to 1850-1899, using the ensemble mean of the ensemble it is plotted against. The applied offset is +0.5ºC for CMIP5 (Figure 3a) and +0.0ºC for CMIP6 (Figure 3b).

Robustness of the regression method. The regression in Fig. 1b was performed on the RACMO2 SSP5-8.5 data (black points). When we include all the reconstructed CESM2 scenarios (blue, yellow, orange and red points in Fig. 1b—see Table A1), the quadratic relation of Equation 1 becomes,

(2) $SMB \sim -14.2\ T^2_{GrIS} - 12.7\ T_{GrIS} + 353$

with an R^2 of 0.83 and an inferred SMB = 0 threshold of 4.6 ± 0.3 ºC, deviating only 0.1 ºC from the result in Fig. 1b. For this reason, we conclude that it is unlikely that

a quantitatively different T_{GrIS} threshold is found when RACMO2 is used to dynamically downscale CESM2 forced with another warming scenario than SSP5-8.5.

Ensemble mean and spread. CMIP5 and CMIP6 ensemble means and standard deviations are calculated arithmetically from the entire ensemble without model weighing. A full list of the exact models used can be found in Tables S3 (CMIP5) and S4 (CMIP6).

Reconstructed SMB and sea level rise estimates from CMIP climate models. The quadratic relationship in Equation 1 is applied to the ensemble mean, and the mean ± one standard deviation. This yields the SMB time series in Fig. S5a, and which are integrated in Fig. S5b. Table S2 uses the ensemble median for consistency with the IPCC.

Extended References

- Dang, C., Zender, C. S., & Flanner, M. G. (2019). Intercomparison and improvement of two-stream shortwave radiative transfer schemes in Earth system models for a unified treatment of cryospheric surfaces. *The Cryosphere*, *13*(9), 2325–2343. https://doi.org/10.5194/tc-13-2325-2019
- Howat, I. M., Negrete, A., & Smith, B. E. (2014). The Greenland Ice Mapping Project (GIMP) land classification and surface elevation data sets. *The Cryosphere*, *8*(4), 1509–1518. https://doi.org/10.5194/tc-8-1509-2014
- van Kampenhout, L., Lenaerts, J. T. M., Lipscomb, W. H., Sacks, W. J., Lawrence, D. M., Slater, A. G., & van den Broeke, M. R. (2017). Improving the Representation of Polar Snow and Firn in the Community Earth System Model. *Journal of Advances in Modeling Earth Systems*, *9*(7), 2583–2600. https://doi.org/10.1002/2017MS000988

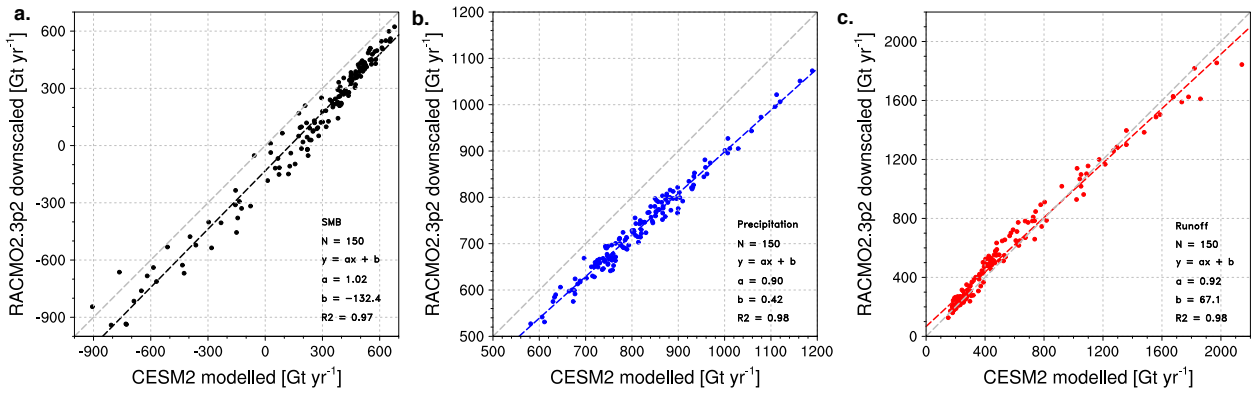

Fig. S1: Cross-model correlation for individual SMB components. Linear correlations between CESM2 SSP5-8.5 and RACMO2 SSP5-8.5 annual GrIS SMB (a), total precipitation (b) and runoff (c), for the period 1950-2100.

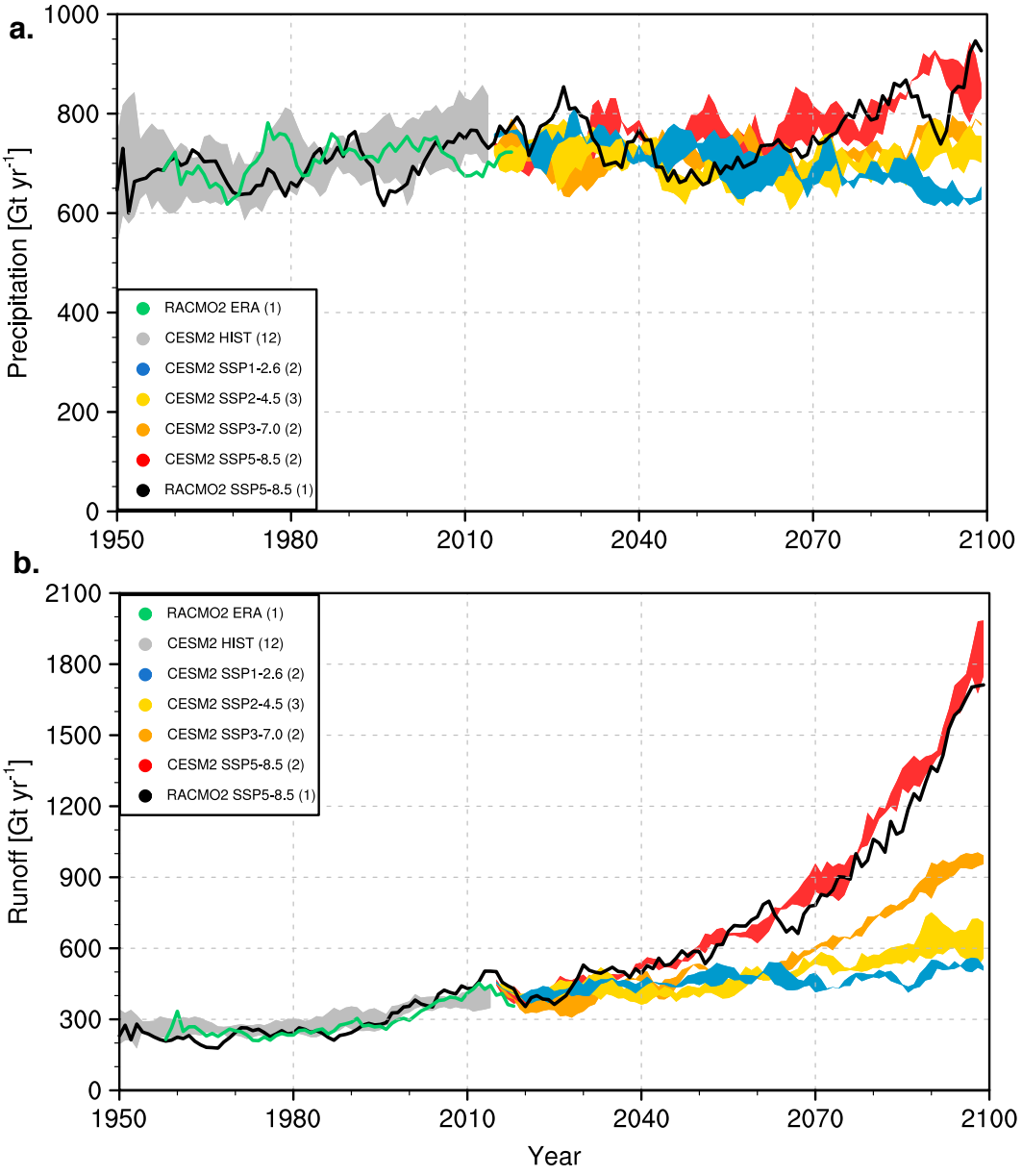

Fig. S2: 21st century Greenland SMB components under various warming scenarios. Five-year simple moving average of GrIS precipitation (a) and runoff (b) for RACMO2 ERA ('observations', green), CESM2 historical (HIST, grey) and scenario runs (colours, see legend). Numbers in parentheses indicate number of ensemble members, coloured bands span maximum and minimum ensemble value. Black line represents RACMO2 SSP5-8.5. See Table A1 for experiment names.

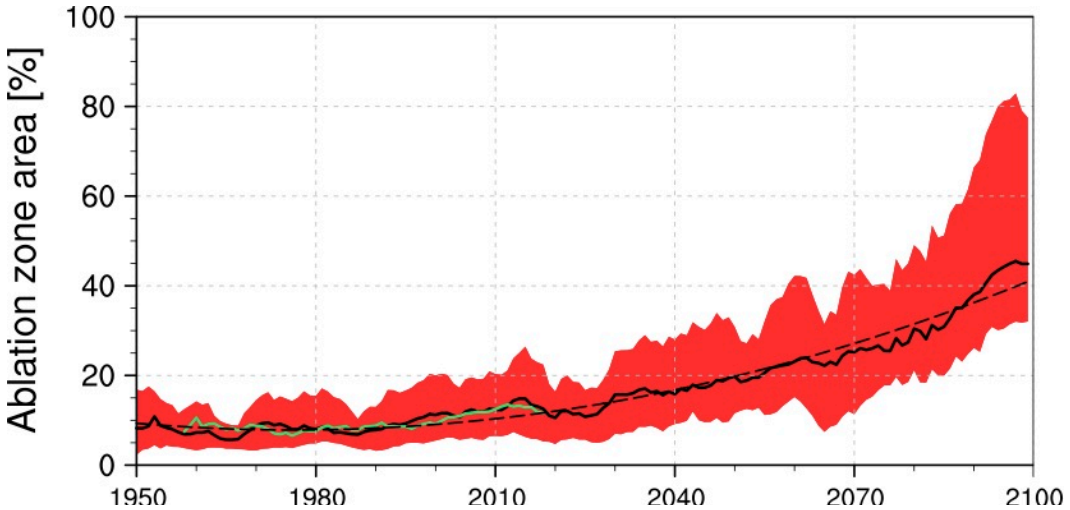

Fig. S3: Non-linear ablation zone expansion. Time series of the ice sheet ablation zone area, i.e. as a fraction of the total land ice area (%), for the period 1950-2100. Black line shows the ice sheet wide ablation zone area while the red band samples the different sectors shown in Fig. 2. The green line shows the RACMO2 ERA simulation for the period 1958-2018 (Noël et al., 2019). Dashed black line shows a quadratic fit.

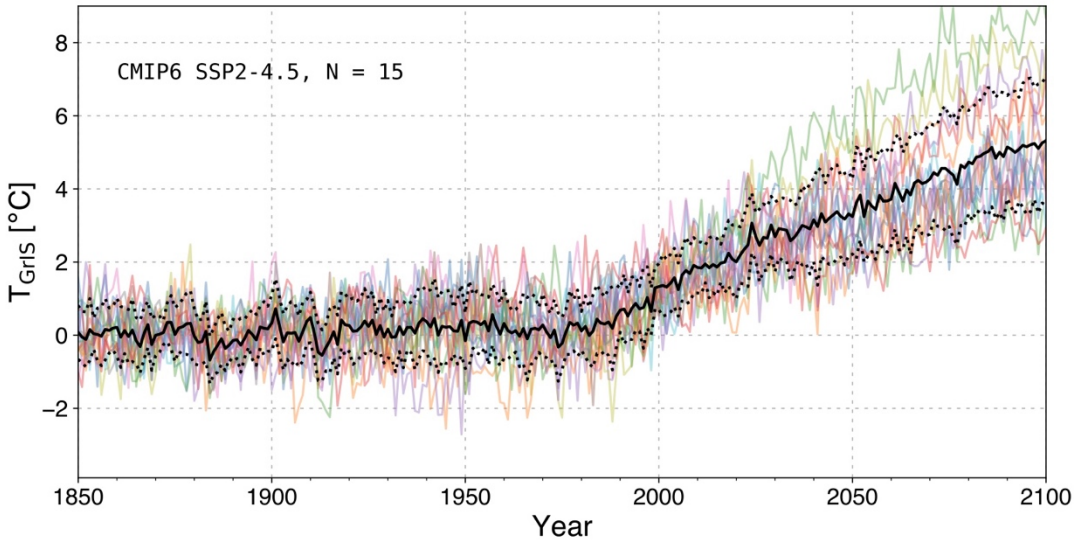

Fig. S4: Anticipated Greenland warming under CMIP6 SSP2-4.5 scenario. Example time series of the anomaly (relative to 1850-1899) of the annual average near-surface temperature averaged over Greenland (T_{GrIS}) in 15 CMIP6 models running the SSP2-4.5 emission scenario. The black solid line indicates the intermodel mean for each year and the dotted lines ± one standard deviation around that.

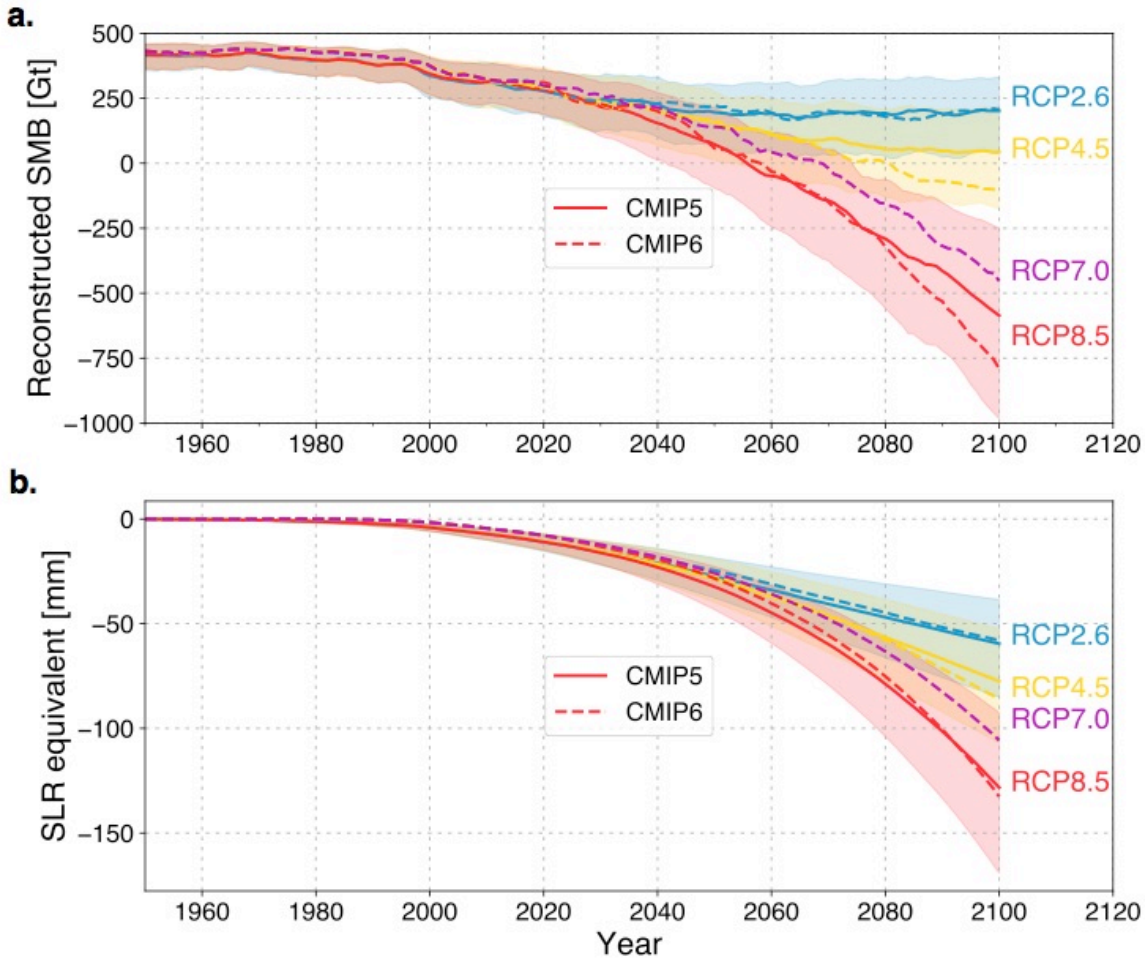

Fig. S5: 21st century contribution from Greenland ice-sheet surface mass balance to sea level rise under multiple warming scenarios. (**a**) Time series of reconstructed GrIS SMB from the SMB-T_{GrIS} relation in Fig. 1b, applied to ensemble mean T_{GrIS} from CMIP5 and CMIP6 models and selected RCP and SSP scenarios. Lines are smoothed with 5-year running mean. Shading indicates ± one standard deviation of the inter-model spread. (**b**) As (**a**), but showing cumulative SMB loss expressed in equivalent sea level rise (assuming a present-day ocean area of 361.9 million km2) with respect to the mean SMB during the period 1900-1950. No smoothing is applied here.

name	period	scenario	ensemble mean	66% likely range
CMIP5	1850-2200	RCP2.6	not reached	-
		RCP4.5	2125	[2037–N/A]
		RCP8.5	2056	[2034–2073]
CMIP6	1850-2100	SSP1-2.6	not reached	-
		SSP2-4.5	2084	[2040–N/A]
		SSP3-7.0	2073	[2041–2087]
		SSP5-8.5	2060	[2039–2079]

Table S1. Estimated year of crossing of the SMB=0 warming threshold. The 66% likely range is calculated from the uncertainties in the temperature threshold (± 0.3 °C) and in the CMIP model spread (± 1 σ). For CMIP5, the period 1850-2200 is considered, and for CMIP6 the period 1850-2100 due to the current unavailability of data.

Scenario	SROCC Table 4.4	This study using CMIP5	This study using CMIP6
RCP 2.6	3 [1 - 7]	5.2 [2.5-8.9]	4.7 [2.0-8.6]
RCP 4.5	4 [1 - 9]	6.6 [3.4-11]	6.5 [3.1-11]
RCP 7.0	n/a	n/a	7.6 [3.5-13]
RCP 8.5	7 [3 - 16]	10.1 [5.8-16]	9.6 [4.5-17]

Table S2. Sea level rise contribution from Greenland SMB. Values are in cm and represent the increase in 2081-2100 relative to 1986-2005 for the various RCP greenhouse gas scenarios. Listed is the ensemble median and *likely* range. Our likely range represents the 5-95 percentile range, which is obtained by scaling the standard deviation by a factor of 1.645, a valid approximation under the assumption that the ensemble spread is normally distributed. SROCC stands for the IPCC Special Report on the Ocean and Cryosphere in a Changing Climate, Oppenheimer et al. (2019).

model	RCP 2.6	RCP 4.5	RCP 8.5
ACCESS1-0		1	1
ACCESS1-3		1	1
bcc-csm1-1	1	1	1
bcc-csm1-1-m	1	1	1
BNU-ESM	1	1	1
CanESM2	1	1	1
CCSM4	1	1	1
CESM1-BGC		1	1
CESM1-CAM5	1	1	1
CESM1-WACCM	1	1	1
CMCC-CESM			1
CMCC-CM		1	1
CMCC-CMS		1	1
CNRM-CM5	1	1	1
CSIRO-Mk3-6-0	1	1	1
CSIRO-Mk3L-1-2		1	
EC-EARTH	1	1	1
FGOALS-g2	1	1	1
FGOALS-s2		1	1
GFDL-CM3	1	1	1
GFDL-ESM2G	1	1	1
GFDL-ESM2M	1	1	1
GISS-E2-H-CC		1	1
GISS-E2-H	1	1	1
GISS-E2-R-CC		1	1
GISS-E2-R	1	1	1
HadGEM2-AO	1	1	1
HadGEM2-CC		1	1
HadGEM2-ES	1	1	1
inmcm4		1	1

IPSL-CM5A-LR	1	1	1
IPSL-CM5A-MR	1	1	1
IPSL-CM5B-LR		1	1
MIROC5	1	1	1
MIROC-ESM-CHEM	1	1	1
MIROC-ESM	1	1	1
MPI-ESM-LR	1	1	1
MPI-ESM-MR	1	1	1
MRI-CGCM3	1	1	1
MRI-ESM1			1
NorESM1-M	1	1	1
NorESM1-ME		1	
	27	40	40

Table S3. Overview of CMIP5 models used in this study. In alphabetical order.

model	**SSP1-2.6**	**SSP2-4.5**	**SSP5-8.5**
BCC-CSM2-MR	1	1	1
CAMS-CSM1-0	1	1	1
CanESM5	1	1	1
CESM2	1	1	1
CESM2-WACCM	1	1	1
CNRM-CM6-1	1	1	1
CNRM-ESM2-1	1	1	1
GFDL-CM4		1	1
GFDL-ESM4	1	1	1
HadGEM3-GC31-LL		1	
IPSL-CM6A-LR	1	1	1
MIROC6	1	1	1
MIROC-ES2L	1	1	1
MRI-ESM2-0	1	1	1
NorESM2-LM	1		1

UKESM1-0-LL	1	1	1
	14	15	15

Table S4. Overview of CMIP6 models used in this study. In alphabetical order.